Oct 19th, 12:00 AM

Finite Element Analysis of Cold-formed Channel Columns

Ben Young

Jintang Yan

Fifteenth International Specialty Conference on Cold-Formed Steel Structures
St. Louis, Missouri U.S.A., October 19-20, 2000

FINITE ELEMENT ANALYSIS OF COLD-FORMED CHANNEL COLUMNS

Ben Young[†] **& Jintang Yan***

ABSTRACT

The paper presents a numerical investigation into the behaviour and strengths of cold-formed plain and lipped channel columns using finite element analysis. A non-linear finite element model is developed and verified against the fixed-ended channel column tests conducted by Young and Rasmussen (1998a, 1998b and 1998c). Geometric and material non-linearities were included in the finite element model. It is demonstrated that the finite element model closely predicted the ultimate loads and the behaviour of the tested cold-formed channel columns. Hence, the model was used for an extensive parametric study of cross-section geometries. Furthermore, the results of the numerical investigation are compared with the design column strengths calculated using the Australian/New Zealand (1996), American (1996) and European (1996) specifications for cold-formed steel structures. It is shown that the design column strengths calculated from the three specifications are generally conservative for plain and lipped channels having maximum plate thickness of 6.0 mm.

1 INTRODUCTION

Cold-formed steel structural members are used increasingly in building construction. The main advantages of cold-formed steel members over the hot-rolled steel members are their superior strength to weight ratio and ease of construction. As a result, the use of cold-formed steel members may lead to a more economic design than hot-rolled steel members. Cold-formed channels are commonly used as compression members such as wall studs and chord members of roof trusses in steel framed residential and commercial buildings. The compression members may fail in local buckling, flexural buckling, flexural-torsional buckling and distortional buckling.

Finite element analysis (FEA) of cold-formed structures plays an increasingly important role in engineering practice, as it is relatively inexpensive and time efficient compared to physical experiments, especially when a parametric study of cross-section geometries is involved. In addition, it is difficult to investigate the effects of geometric imperfections and residual stresses of structural members experimentally. Therefore, FEA is more economical than physical experiments, provided that the finite element model (FEM) is accurate. Hence, it is necessary to verify the FEM with experimental results. In general, FEA is a powerful tool in predicting the ultimate loads and complex failure modes of cold-formed structural members. In addition, local and overall geometric imperfections, residual stresses and material non-linearity can be included in the FEM.

†, * School of Civil and Structural Engineering, Nanyang Technological University, Singapore 639798.

The purpose of the paper is to develop an accurate FEM to investigate the behaviour and strengths of fixed-ended cold-formed plain and lipped channel columns. The finite element analysis program ABAQUS (1998) was used for the numerical investigation. The FEM was verified against the column tests conducted by Young and Rasmussen (1998a, 1998b and 1998c). The FEM included geometric and material non-linearities. A sensitivity analysis on geometric imperfections of the columns was performed to determine the most appropriate scale factor for the FEM. The verified model was then used for an extensive parametric study of cross-section geometries. The maximum plate thickness of the channel sections is 6.0 mm having the flange width to thickness of 13.3. Hence, these channel sections are considered to be stocky. In addition, column strength equation based on the results obtained from FEA is proposed. The column strengths obtained from the proposed equation are compared with the design column strengths calculated using the Australian/New Zealand, American and European specifications for cold-formed steel structures. The reliability of the proposed equation is evaluated using reliability analysis.

2 SUMMARY OF TEST PROGRAM

The test program described in Young and Rasmussen (1998a, 1998b and 1998c) provided experimental ultimate loads and failure modes for cold-formed plain and lipped channel columns compressed between fixed ends and pinned ends. The test specimens were brake-pressed from high strength zinc-coated grade G450 structural steel sheets having nominal yield stress of 450 MPa and specified according to the Australian Standard AS 1397 (1993). The test program comprised four different cross-section geometries, two series of plain channels and two series of lipped channels. The four channel sections had a nominal thickness of 1.5 mm and a nominal width of the web of 96 mm. The nominal width of the lip of both lipped channels was 12 mm. The nominal flange width was either 36 mm or 48 mm and was the only variable in the cross-section geometry. Accordingly, the four test series were labeled P36, P48, L36 and L48 where "P" and "L" refer to "plain" and "lipped" channels respectively. The average values of measured cross-section dimensions of the fixed-ended test specimens are shown in Table 1 using the nomenclature defined in Fig. 1. The specimens were tested at various column lengths ranging from 280 mm to 3500 mm. The measured cross-section dimensions of each specimen are detailed in Young and Rasmussen (1998a, 1998b and 1998c).

The material properties determined from coupon tests are summarised in Table 2. The table contains the nominal and the measured static 0.2% tensile proof stress ($\sigma_{0.2}$), the static 0.5% tensile proof stress ($\sigma_{0.5}$), and the static ultimate tensile strength (σ_u) as well as the Young's modulus (E) and the elongation after fracture (ε_u) based on a gauge length of 50 mm. The coupons were taken from the centre of the web plate in the longitudinal direction of the finished specimens. The coupon dimensions conformed to the Australian Standard AS1391 (1991) for the tensile testing of metals using 12.5 mm wide coupons of gauge length 50 mm. The coupons were tested in an Instron TT-KM 250 kN capacity displacement controlled testing machine using friction grips to apply loading at a constant speed of 1 mm/min. The static load was obtained by pausing the applied straining for one minute near the 0.2% proof stress and the ultimate tensile strength. This allowed the stress relaxation associated with plastic straining to take place. The stress-strain curves obtained from the coupon tests are detailed in Young and Rasmussen (1998a and 1998b).

Residual stress measurements of the lipped channel specimens from Series L48 were obtained by Young and Rasmussen (1995b). The *membrane* and the *flexural* residual stresses were

found to be less than 3% and 7% of the measured 0.2% tensile proof stress respectively. Hence, the residual stresses were deemed negligible compared with the 0.2% tensile proof stress.

Local and overall geometric imperfections were measured prior to testing for the tested columns. The measured maximum local imperfections were found to be of the order of the plate thickness at the tip of the flanges for all test series. For the fixed-ended specimens, the maximum overall minor axis flexural imperfections at mid-length were 1/1400, 1/2500, 1/1100 and 1/1300 of the specimen length for Series P36, P48, L36 and L48 respectively. The measured local and overall geometric imperfection profiles are detailed in Young and Rasmussen (1995a and 1995b).

A 250 kN servo-controlled hydraulic actuator was used to apply compressive axial force to the specimen. The tests were controlled by incrementing the shortening of the specimen. This allowed the tests to be continued into the post-ultimate range. Readings of the applied load were taken approximately one minute after applying an increment of compression, hence allowing the stress relaxation associated with plastic straining to take place. Consequently, the loads recorded were considered to be static loads. The fixed-ended bearings were designed to restrain both minor and major axis rotations as well as twist rotations and warping. Details of the test rig are given in Young and Rasmussen (1998d and 1999). The experimental ultimate loads (P_{Exp}) of the test specimens are shown in Tables 3-4 and 7-10. The test specimens were labeled such that the test series, type of boundary conditions and specimen length could be identified from the label. For example, the label "P36F0280" defines the specimen belongs to the test Series P36, the fourth letter "F" indicates that the specimen is fixed-ended, and the last four digits are the specimen length of 280 mm.

3 NUMERICAL INVESTIGATION

3.1 Development and Verification of Finite Element Model

3.1.1 General

The finite element non-linear analysis program ABAQUS (1998) version 5.8 was used to simulate the experimental behaviour of fixed-ended cold-formed plain and lipped channel columns. The numerical simulation consisted of two stages. In the first stage, an eigenvalue elastic buckling analysis, also known as linear perturbation analysis, was performed on a "perfect" geometry to establish probable buckling modes of the column. In the second stage, a non-linear analysis by incorporating both geometric and material non-linearities was then performed using the modified Riks method (ABAQUS, 1998) to obtain the ultimate load and failure modes of the column.

In the finite element model (FEM), the experimental measured cross-section dimensions, base metal thickness, material properties and initial geometric imperfections were modeled. However, the residual stresses and the rounded corners of the channel sections were not included in the model. This is due to the small values of the measured *membrane* and *flexural* residual stresses were less than 3% and 7% of the proof stress ($\sigma_{0.2}$) respectively, as well as a small value of the measured inside corner radius of 0.85 mm as reported by Young and Rasmussen (1995b and 1998b).

3.1.2 Element Type and Mesh

The S4R5 thin shell elements were used in the FEM. The S4R5 element is a four-node doubly curved shell element with reduced integration and hourglass control using five degrees of freedom per node (ABAQUS, 1998). The finite element mesh used in the model was investigated by varying the aspect ratio (length to width) of the elements in the cross-section. It was found that good simulation results could be obtained by using the aspect ratios of approximately 1.7, 1.1 and 0.8 for the lip, flange and web elements respectively. The sizes of the elements are approximately 10 mm × 6 mm (length by width), 10 mm × 9 mm and 10 mm × 12 mm for the lip, flange and web elements respectively. The length of the elements in the FEM was 10 mm. Typical finite element meshes of plain and lipped channels are shown in Figs 2 and 3 respectively.

3.1.3 Boundary Condition

The FEM simulated the channel columns compressed between fixed ends. The fixed-ended boundary condition was modeled by restraining all the degrees of freedom of the nodes at both ends, except for the translational degree of freedom in the axial direction at the top end of the column. This is due to the load applied at the top end of the column. The nodes other than the two ends were free to translate and rotate in any directions.

3.1.4 Method of Loading

The loading method used in the finite element analysis (FEA) is identical to that used in the tests. The displacement control method was used for the analysis of the columns. Axial compressive load was applied to the column by specifying a displacement to the nodes at the top end of the column. Generally, a displacement of 6 mm was specified, and the displacement is equivalent to the axial shortening of the column.

3.1.5 Material Properties

As mentioned earlier, the first stage of the numerical simulation is a linear analysis in which there is a linear relationship between the applied loads and the response of the structure. In this analysis, the stiffness of the structure remained unchanged. Hence, only the density, Young's modulus and Poisson's ratio defined the material properties. However, the second stage of the numerical simulation is a non-linear analysis in which the stiffness of the structure changed as it deformed. The material non-linearity was included in the FEM by specifying the true values of stresses and strains. The plasticity of the material was simulated by a mathematical model, known as the incremental plasticity model, and the true stress (σ_{true}) and true plastic strain (ε^{pl}_{true}) were calculated as (ABAQUS, 1998),

$$\sigma_{true} = \sigma(1+\varepsilon) \tag{1}$$

$$\varepsilon^{pl}_{true} = \ln(1+\varepsilon) - \sigma_{true}/E \tag{2}$$

where E is the Young's modulus, σ and ε are the measured engineering stress and strain based on the original cross-section area of the coupon specimens as detailed in Young and Rasmussen (1998a and 1998b). The stresses and strains were obtained from the coupon specimens loaded at a constant speed of 1 mm/min. The incremental plasticity model required

only the non-linear range of the true stress-strain curve. The non-linear range includes the portion from the end of the linear range to the ultimate point of the true stress-strain curve.

3.1.6 Geometric Imperfections and Sensitivity Analysis

The geometric imperfections were included in the FEM by using a linear perturbation analysis. The main purpose of the perturbation analysis is to establish probable buckling modes (eigenmode) of the column. The eigenmode was then scaled by a factor (scale factor) to obtain a perturbed mesh for the non-linear analysis. Eigenmode 1 was used in the FEM. Typical buckling (eigenmode 1) of plain and lipped channels are shown in Figs 2 and 3 respectively.

A sensitivity analysis on geometric imperfections of the columns was performed for the test Series P36 to determine the most appropriate scale factor for the FEM. A series of scale factors expressed in terms of 100%, 75%, 50%, 25%, 5%, 2%, and 0.02% of the measured geometric imperfections and the plate thickness were investigated. The results of the sensitivity analysis are shown in Tables 3-4 and 5-6 for the column strengths and the axial shortenings respectively. In Tables 3-6, P_{EXP} is the experimental ultimate load, P_{FEA} is the ultimate load predicted by the FEA, P_{FEA}^{*} is the proposed ultimate load obtained from Eqn. 3, e_{EXP} and e_{FEA} are the axial shortening at ultimate load obtained from the tests and FEA respectively. The results of the sensitivity analysis obtained based on the measured geometric imperfections are similar to those based on the plate thickness. Therefore, the scale factors used in the parametric study are based on the plate thickness of the sections. It is shown that the scale factors of 25%, 5% and 2% of the measured geometric imperfections and the plate thickness are relatively close and provided good predictions compared to the experimental data. Generally, the column strength predictions using a scale factor of 25% of the plate thickness were conservative for test Series P36, as shown in Table 4. The scale factor of 25% of the plate thickness was chosen for the parametric study.

3.1.7 Comparison of Experimental Results with Finite Element Analysis Results

The developed FEM based on the test Series P36 was further verified against the experimental results of test Series P48, L36, and L48. The non-linear range of the true stress-strain curves for the corresponding test series were used in the FEM. A scale factor of 25% of the plate thickness of the sections was used in modeling the geometric imperfections of the columns. The ultimate loads, axial shortenings and failure modes at ultimate load predicted by the FEA are compared with the experimental results of plain and lipped channel columns as shown in Tables 7-10.

The ultimate loads (P_{FEA}) predicted by the FEA are compared with the experimental ultimate loads (P_{EXP}) as shown in Tables 7, 8, 9 and 10 for Series P36, P48, L36 and L48 respectively. Tables 7-10 show the experimental-to-FEA ultimate load ratios (P_{EXP}/P_{FEA}) for the comparison. In general, it is shown that the ultimate loads predicted by the FEA slightly overestimated the experimental ultimate loads. The mean values of the experimental-to-FEA ultimate load ratio of 0.93, 1.00, 0.97 and 0.99 with the corresponding coefficient of variation (COV) of 0.076, 0.080, 0.051 and 0.057 for Series P36, P48, L36 and L48 respectively are shown in Tables 7-10.

The axial shortenings (e_{FEA}) at ultimate load predicted by the FEA are also compared with the experimental axial shortenings (e_{EXP}) as shown in Tables 7-10. It is found that most of the axial shortenings predicted by the FEA overestimated the experimental values for Series P36, P48

and L36. However, the axial shortenings are conservatively predicted by the FEA for Series L48, except for specimens L48F1500 and L48F2000.

The failure modes at ultimate load obtained from the tests and FEA are shown in Tables 7-10. Four failure modes were observed, including the local buckling (L), distortional buckling (D), minor axis flexural buckling (F) and flexural-torsional buckling (FT) modes. Generally, the failure modes predicted by the FEA were in good agreement with the failure modes observed in the tests. For plain channel columns, flexural-torsional buckling mode was predicted by the FEA instead of flexural buckling mode as observed in the test for specimen P36F2500. The test specimen P48F3000 failed in local, flexural and flexural-torsional buckling modes, however flexural-torsional buckling was not predicted by the FEA. For lipped channel columns, flexural-torsional buckling mode was not predicted by the FEA for intermediate column lengths (1500 mm and 2000 mm). The test specimen L48F2000 failed in local, distortional and flexural-torsional buckling modes, however local and flexural buckling modes were predicted by the FEA.

Load versus axial shortening curves predicted by the FEA are compared with the experimental curves as shown in Figs 4 and 5 for specimen P48F2500 having a column length of 2500 mm and specimen L48F1000 having a column length of 1000 mm respectively. It is shown that the load-shortening curves predicted by the FEA follow closely the experimental curves. Figs 6a and 7a show the buckling of the tested columns for specimens P48F1850 and L48F0300 respectively. Specimen P48F1850 failed in combined local and flexural buckling modes, and specimen L48F0300 failed in combined local and distortional buckling modes. Figs 6b and 7b show the deformed shapes of the corresponding specimens predicted by the FEA. The deformed shapes obtained from the FEA closely simulated the experimental buckling modes. The resemblance of Figs 6a and 6b, and Figs 7a and 7b demonstrates the reliability of the FEA predictions. ABAQUS/Post (1998) was used to generate the load-shortening curves and the deformed shapes of the columns.

3.1.8 Proposed Column Strength Equation

Generally, the ultimate loads (P_{FEA}) predicted by the FEA slightly overestimated the experimental ultimate loads (P_{EXP}), as shown in Tables 7-10. This is probably due to the small values of residual stresses and the rounded corners of the sections that were ignored in the FEM. Hence, column strength equation based on the ultimate loads (P_{FEA}) predicted by the FEA, the column lengths and the test results is proposed.

The proposed column strength equation for plain and lipped channels is,

$$P_{FEA}^{*} = (C - 0.02L)P_{FEA} \tag{3}$$

where P_{FEA}^{*} is the proposed column strength, P_{FEA} is the ultimate load predicted by the FEA, L is the column length in meters, and C is a calibration factor that was obtained from the calibration of the test results of Series P36, P48, L36 and L48. The calibration factor for plain and lipped channel columns are 0.95 and 1.00 respectively.

3.1.9 Comparison of Test Strengths with Proposed Column Strengths

The proposed column strengths (P_{FEA}^*) obtained from Eqn. 3 are compared with the experimental ultimate loads (P_{EXP}) as shown in Tables 7-10. The ratios of the test strength to the proposed column strength (P_{EXP}/P_{FEA}^*) were calculated. The proposed column strengths are generally conservative for the tested plain and lipped channel columns. The mean values of the test strength to the proposed column strength (P_{EXP}/P_{FEA}^*) ratio of 1.02, 1.08, 1.01 and 1.03 with the corresponding coefficient of variation of 0.075, 0.099, 0.052 and 0.075 for Series P36, P48, L36 and L48 respectively are shown in Tables 7-10.

4 PARAMETRIC STUDY

It has been shown that the FEM closely predicted the column strengths and the behaviour of the tested channels. Hence, the model was used for an extensive parametric study of cross-section geometries. In the parametric study, a total of 108 specimens consisting of eighteen different cross-section geometries of cold-formed plain and lipped channel columns compressed between fixed ends were investigated.

Nine series of plain channels and nine series of lipped channels having a flange width of 80 mm and the width of the lip of 15 mm were studied. The width of the web was 100 mm, 150 mm and 200 mm, and the plate thickness was 1.5 mm, 3.0 mm and 6.0 mm. The flange width to thickness ratio ranged from 13.3 to 53.3. The series were labeled such that the type of channels, plate thickness and the width of the web could be identified from the label. For example, the label "P1.5W100" defines the series as follows:

- The first letter "P" indicates a plain channel, where "L" indicates a lipped channel.
- The next two digits (1.5) refer to the plate thickness of the section in mm (1.5 mm).
- The notation "W100" indicates the width of the web in mm (100 mm).

The column length ranged from 500 mm to 3000 mm at an increment of 500 mm.

The material properties of the plain and lipped channels used in the parametric study are identical to those used in the FEA for the test Series P36 and L36 respectively. A scale factor of 25% of the plate thickness of the sections was used in modeling the geometric imperfections of the columns. The finite element mesh was slightly modified to cater for the new cross-section dimensions of the specimens. The aspect ratios (length to width) of 1.3, 1.0 and 1.0 for the lip, flange and web elements respectively were used. The sizes of the elements are 10 mm × 7.5 mm (length by width), 10 mm × 10 mm and 10 mm × 10 mm for the lip, flange and web elements respectively.

The proposed column strengths (P_{FEA}^*) obtained from the FEA are plotted against the *effective* length for minor axis flexural buckling (l_{ey}) in Figs 8-25. The effective length (l_{ey}) was assumed equal to one-half of the column length for the fixed-ended columns ($l_{ey} = L/2$). The failure modes at ultimate load obtained from the FEA are also shown in Figs 8-25. The theoretical minor axis flexural buckling loads and flexural-torsional buckling loads of the fixed-ended columns are shown in Figs 8-25. The theoretical flexural and flexural-torsional buckling loads are summarised in Young and Rasmussen (1995a). In calculating the flexural-torsional buckling loads, the effective lengths for major axis flexure and warping were taken as one-half of the column length for the fixed-ended columns, because the major axis rotations and warping were restrained.

5 COMPARISON OF PROPOSED COLUMN STRENGTHS WITH DESIGN COLUMN STRENGTHS

The proposed column strengths (P_{FEA}^*) obtained from the FEA in the parametric study are compared with the unfactored design column strengths calculated using the Australian/New Zealand (AS/NZS 4600, 1996), American (AISI, 1996) and European (EC 3, 1996) specifications for cold-formed steel structures, as shown in Figs 8-25 and Tables 11-12. The design column strengths were calculated using the material properties as those used in the FEA of the parametric study. Hence, the material properties of Series P36 and L36 were used for plain and lipped channels respectively, as shown in Table 2. In calculating the design column strengths, the effective lengths for minor and major axes flexure, and warping were taken as one-half of the column length, and the fixed-ended columns are designed as concentrically loaded compression members as recommended by Young and Rasmussen (1998a and 1998b). In the compression member design rules, the AS/NZS 4600 includes a separate check for distortional buckling of singly-symmetric sections as specified in Clause 3.4.6. In the calculation of the distortional buckling loads using Clause 3.4.6, the elastic distortional buckling stresses (f_{od}) were obtained from Appendix D of the AS/NZS 4600. The distortional buckling loads for lipped channel columns are shown in Figs 17-25.

For plain channel columns, the design column strengths calculated using the three specifications are generally conservative, as shown in Figs 8-16. The EC 3 design strengths are less conservative than the AS/NZS and AISI design strengths for channels having plate thickness of 1.5 mm, however it is more conservative for channels having plate thickness of 3.0 mm and 6.0 mm. The EC 3 design strengths are slightly unconservative at an effective length of 1500 mm for Series P1.5W150, P1.5W200 and P3.0W200. For channels having plate thickness of 3.0 mm and 6.0 mm, the EC 3 design strengths are slightly unconservative at the shortest effective length (l_{ey} = 250 mm) for Series P6.0W150, and at short effective lengths (l_{ey} ≤ 500 mm) for Series P6.0W200. The AS/NZS and AISI design strengths are slightly unconservative at an effective length of 1500 mm for Series P3.0W150, P3.0W200 and P6.0W100, and at an effective length of 1250 mm for Series P3.0W200. The AS/NZS and AISI design strengths are unconservative for Series P6.0W200 with a maximum deviation of 7%, except for the longest column (l_{ey} = 1500 mm). For Series P6.0W150, the AS/NZS and AISI design strengths are unconservative at short effective lengths.

For lipped channel columns, the design strengths calculated using the three specifications are generally conservative, as shown in Figs 17-25. The EC 3 design strengths are conservative for all channel columns. It is found that the EC 3 design strengths are more conservative than the AS/NZS and AISI design strengths for all channels. For channels having plate thickness of 1.5 mm, the AS/NZS and AISI design strengths are unconservative at intermediate (500 mm < l_{ey} ≤ 1000 mm) and long (l_{ey} > 1000 mm) effective lengths for Series L1.5W150 and L1.5W200. The AISI design strength is slightly unconservative at an effective length of 500 mm for Series L1.5W200, while the AS/NZS accurately calculated the design strength. This is a result of the fact that the AS/NZS contains design rules specifically for distortional buckling. The AS/ZNS and AISI design strengths are conservative for all channels having plate thickness of 3.0 mm. For channels having plate thickness of 6.0 mm, the AS/ZNS and AISI design strengths are slightly unconservative at an effective length of 1500 mm for Series L6.0W100 and L6.0W150, and at an effective length of 1250 mm for Series L6.0W100. The AS/ZNS and AISI design strengths are slightly unconservative at short and intermediate effective lengths for Series L6.0W200, except that the AS/NZS accurately calculated the design strengths at short effective lengths for distortional buckling of the channels.

Tables 11 and 12 show the mean values of the proposed column strengths to the unfactored design column strengths $P_{FEA}^*/P_{AS/NZS}$, P_{FEA}^*/P_{AISI} and P_{FEA}^*/P_{EC3} ratios with the corresponding coefficients of variation (COV) for Australian/New Zealand, American and European specifications respectively. Six columns at various lengths were investigated for each series. For plain channel columns, the mean values of $P_{FEA}^*/P_{AS/NZS}$ ratio ranged from 0.97 to 1.22 with the COV ranged from 0.033 to 0.056, and the mean values of P_{FEA}^*/P_{EC3} ratio ranged from 1.03 to 1.15 with the COV ranged from 0.028 to 0.118. For lipped channel columns, the mean values of $P_{FEA}^*/P_{AS/NZS}$ ratio ranged from 0.97 to 1.13 with the COV ranged from 0.020 to 0.093, and the mean values of P_{FEA}^*/P_{AISI} ratio ranged from 0.96 to 1.11 with the COV ranged from 0.014 to 0.078. The mean values of P_{FEA}^*/P_{EC3} ratio ranged from 1.08 to 1.25 with the COV ranged from 0.014 to 0.095.

6 RELIABILITY ANALYSIS

The reliability of the proposed column strength equation based on the results obtained from FEA is evaluated using reliability analysis. The reliability or safety of the proposed equation is measured by a safety index (β). A target safety index of 2.5 for cold-formed structural members is recommended by the AISI Specification. In general, the proposed equation is considered to be reliable if the safety index is greater than 2.5. The existing resistance (capacity) factor (ϕ) of 0.85 for concentrically loaded compression members is given by the Australian/New Zealand (AS/NZS 4600, 1996) and American (AISI, 1996) specifications, while a ϕ factor of 1/1.1 is given by the European (EC 3, 1996) specification for cold-formed steel structures. These ϕ factors are used in the reliability analysis. The safety index may be calculated as,

$$\beta = \frac{\ln\left(\frac{M_m F_m P_m}{L_C \phi}\right)}{\sqrt{\left(V_M^2 + V_F^2 + C_P V_P^2 + 0.21^2\right)}} \tag{4}$$

The load combinations of 1.25DL + 1.50LL, 1.2DL +1.6LL and 1.35DL + 1.5 LL are used in the analysis for AS/NZS, AISI and EC 3 specifications respectively, where DL is the dead load and LL is the live load. According to Rogers and Hancock (1996), the load combination factor (L_C) in Eqn. 4 is calculated as 0.691, 0.657 and 0.683 for AS/NZS, AISI and EC 3 specifications respectively. The statistical parameters M_m, F_m, V_M and V_F are the mean values and coefficients of variation for material properties and fabrication variables. These values are obtained from Table F1 of the AISI (1996) Specification for concentrically loaded compression members, where M_m = 1.10, F_m = 1.00, V_M = 0.10 and V_F =0.05. The statistical parameters P_m and V_P for the proposed column strength equation are the mean value and coefficient of variation respectively, as shown in Tables 7-12. The correction factor C_P is used to account for the influence due to a small number of specimens (Peköz and Hall 1988, and Tsai 1992), and the factor C_P is given in Eqn. F1.1-3 of the AISI (1996) Specification. Equation 4 is detailed in Rogers and Hancock (1996).

Tables 7-12 show the safety indices (β) of the proposed column strength equation based on the results obtained from FEA are generally higher than the target value (β = 2.5). Therefore, it is shown that the FEA predictions are reliable.

7 CONCLUSIONS

A numerical investigation of fixed-ended cold-formed plain and lipped channel columns using finite element analysis has been presented. A finite element model including geometric and material non-linearities has been developed and verified against experimental results. The failure modes at ultimate load predicted by the finite element analysis were generally in good agreement with the failure modes observed in the tests, whereas the axial shortenings at ultimate load predicted by the finite element analysis overestimated the experimental values. The finite element model closely predicted the experimental ultimate loads of the channel columns. However, the finite element analysis predictions slightly overestimated the experimental ultimate loads. Hence, column strength equation based on the results obtained from finite element analysis has been proposed. The proposed column strengths were compared with the test strengths. Generally, the proposed column strengths were conservative for the plain and lipped channel columns.

An extensive parametric study of cross-section geometries has been performed using the developed finite element model. The plate thickness of the channel sections ranged from 1.5 mm to 6.0 mm, and the flange width to thickness ratio ranged from 13.3 to 53.3. The column length ranged from 500 mm to 3000 mm. A comparison of the proposed column strengths obtained from the finite element analysis, and the design column strengths calculated using the Australian/New Zealand (1996), American (1996) and European (1996) specifications for cold-formed steel structures has been presented. It has been shown that the design column strengths calculated from the three specifications were generally conservative for plain and lipped channel columns. The reliability of the proposed column strength equation based on the results obtained from finite element analysis has been evaluated using reliability analysis. The safety indices of the proposed column strength equation are generally higher than the target safety index of 2.5 as specified in the AISI Specification. Therefore, it has been shown that the finite element analysis predictions are reliable.

REFERENCES

ABAQUS Standard User's Manual. (1998). Hibbitt, Karlsson and Sorensen, Inc., Vol. 1, 2 and 3, Version 5.8, USA.

ABAQUS Post Manual. (1998). Hibbitt, Karlsson and Sorensen, Inc., Version 5.8, USA.

American Iron and Steel Institute. (1996). *Specification for the Design of Cold-Formed Steel Structural Members*. AISI, Washington, DC.

Australian Standard. (1991). *Methods for Tensile Testing of Metals*. AS 1391, Standards Association of Australia, Sydney, Australia.

Australian Standard. (1993). *Steel Sheet and Strip -- Hot-dipped zinc-coated or aluminium/zinc-coated*. AS 1397, Standards Association of Australia, Sydney, Australia.

Australian/New Zealand Standard. (1996). *Cold-Formed Steel Structures*. AS/NZS 4600:1996, Standards Australia, Sydney, Australia.

Eurocode 3. (1996). *ENV 1993-1-3, Design of Steel Structures, Part 1.3: Supplementary Rules for Cold-Formed Thin Gauge Members and Sheeting.* EC 3, Draft February 1996, CEN, Brussels, Belgium.

Peköz, T.B., and Hall, W.B. (1988). "Probabilistic Evaluation of Test Results." Proceedings of the 9th International Specialty Conference on Cold-Formed Steel Structures, St. Louis, University of Missouri-Rolla, Mo, USA.

Rogers, C.A., and Hancock, G.J. (1996). "Ductility of G550 Sheet Steels in Tension-Elongation Measurements and Perforated Tests." *Research Report* R735, Department of Civil Engineering, University of Sydney, Australia.

Tsai, M. (1992). *Reliability Models of Load Testing.* PhD dissertation, Department of Aeronautical and Astronautical Engineering, University of Illinois at Urbana-Champaign.

Young, B., and Rasmussen, K.J.R. (1995a). "Compression Tests of Fixed-ended and Pin-ended Cold-Formed Plain Channels." *Research Report* R714, School of Civil and Mining Engineering, University of Sydney, Australia.

Young, B., and Rasmussen, K.J.R. (1995b). "Compression Tests of Fixed-ended and Pin-ended Cold-Formed Lipped Channels." *Research Report* R715, School of Civil and Mining Engineering, University of Sydney, Australia.

Young, B., and Rasmussen, K.J.R. (1998a). "Tests of Fixed-ended Plain Channel Columns." *Journal of Structural Engineering,* ASCE, 124(2), 131-139.

Young, B., and Rasmussen, K.J.R. (1998b). "Design of Lipped Channel Columns." *Journal of Structural Engineering,* ASCE, 124(2), 140-148.

Young, B., and Rasmussen, K.J.R. (1998c). "Tests of Cold-Formed Channel Columns." Proceedings of the 14th International Specialty Conference on Cold-Formed Steel Structures, St. Louis, University of Missouri-Rolla, Mo, USA, 239-264.

Young, B., and Rasmussen, K.J.R. (1998d). "Behaviour of Locally Buckled Singly Symmetric Columns." Proceedings of the 14th International Specialty Conference on Cold-Formed Steel Structures, St. Louis, University of Missouri-Rolla, Mo, USA, 219-238.

Young, B., and Rasmussen, K.J.R. (1999). "Behaviour of Cold-formed Singly Symmetric Columns." *Thin-walled Structures,* 33(2), 83-102.

NOTATION

A	Full cross-section area
B_f	Overall width of flange
B_l	Overall width of lip
B_w	Overall width of web
C	Calibration factor of proposed column strength equation
COV	Coefficient of variation
C_p	Correction factor in reliability analysis

DL	Dead load
E	Young's modulus of elasticity
e	Axial shortening
e_{EXP}	Experimental axial shortening at ultimate load
e_{FEA}	Axial shortening at ultimate load obtained from FEA
FEA	Finite element analysis
FEM	Finite element model
F_m	Mean value of fabrication variables
f_{od}	Elastic distortional buckling stress
L	Column length
LL	Live load
L_C	Load combination factor in reliability analysis
l_{ey}	Effective length for minor axis flexural buckling
M_m	Mean value of material properties
P_{AISI}	Unfactored design column strength calculated using American specification
$P_{AS/NZS}$	Unfactored design column strength calculated using Australian/New Zealand specification
P_{EC3}	Unfactored design column strength calculated using European specification
P_{Exp}	Experimental ultimate load
P_{FEA}	Ultimate load predicted by FEA
P_{FEA}^*	Proposed column strength obtained from FEA
P_m	Mean value of proposed column strength equation
P_u	Ultimate load
r_i	Inside corner radius of specimen
t	Plate thickness
t^*	Base metal thickness
V_F	Coefficient of variation of fabrication variables
V_M	Coefficient of variation of material properties
V_P	Coefficient of variation of proposed column strength equation
x	In-plane transverse coordinate
y	Out-of-plane transverse coordinate
β	Safety index (Reliability index)
ε	Measured engineering strain
ε_u	Elongation (tensile strain) after fracture based on a gauge length of 50mm
ε_{true}^{pl}	True plastic strain
σ	Measured engineering stress
$\sigma_{0.2}$	Static 0.2% tensile proof stress
$\sigma_{0.5}$	Static 0.5% tensile proof stress
σ_{true}	True stress
σ_u	Static ultimate tensile strength
ϕ	Resistance (capacity) factor

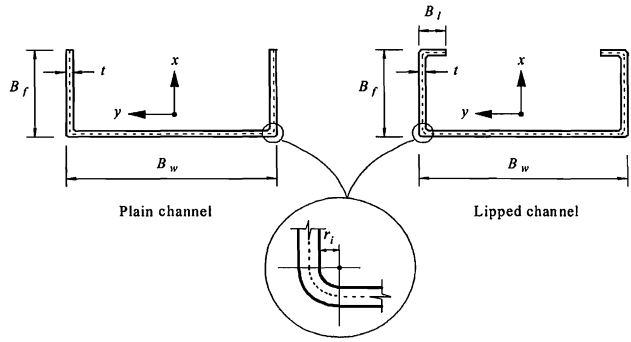

Fig. 1. Definition of Symbols

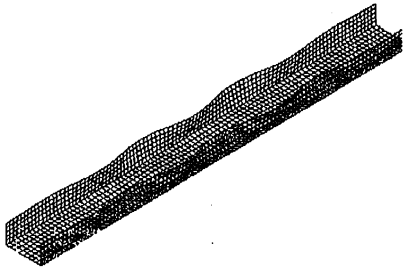

Fig. 2. Typical Finite Element Mesh and Buckling (Eigenmode 1) of Plain Channel

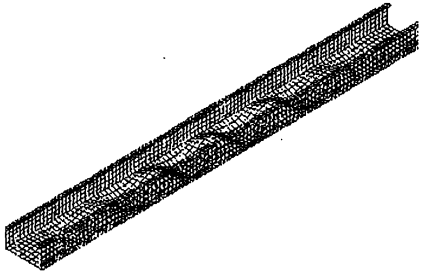

Fig. 3. Typical Finite Element Mesh and Buckling (Eigenmode 1) of Lipped Channel

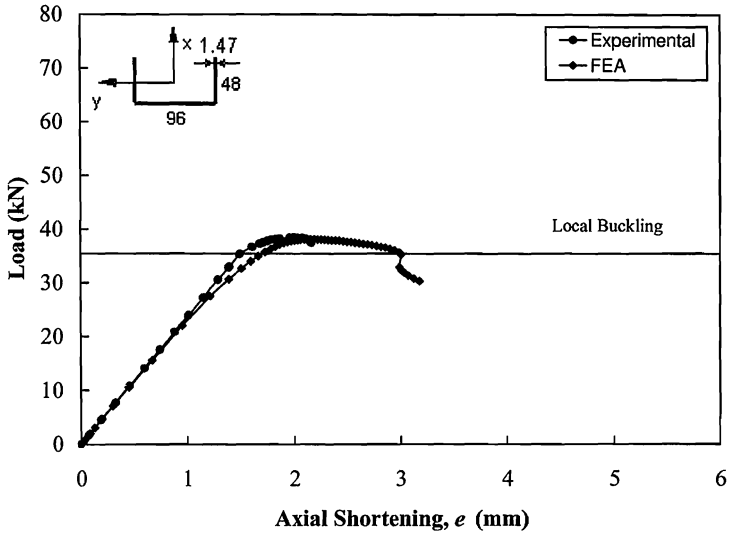

Fig. 4. Comparison of Experimental and FEA Load Versus Axial Shortening Curves for Specimen P48F2500

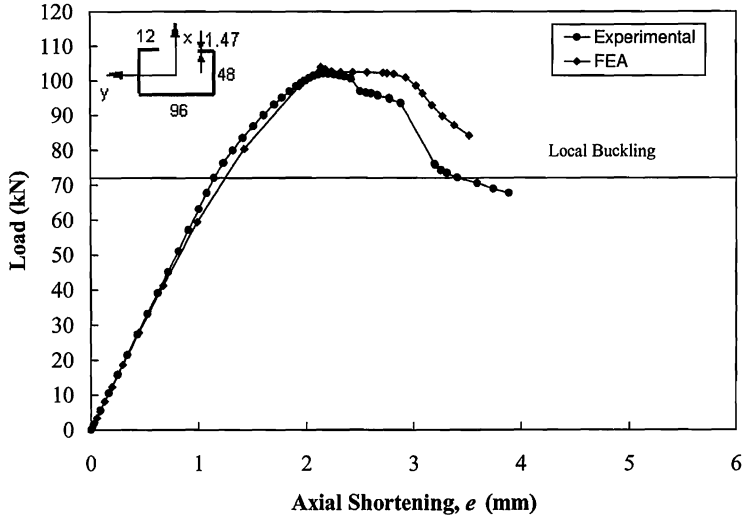

Fig. 5. Comparison of Experimental and FEA Load Versus Axial Shortening Curves for Specimen L48F1000

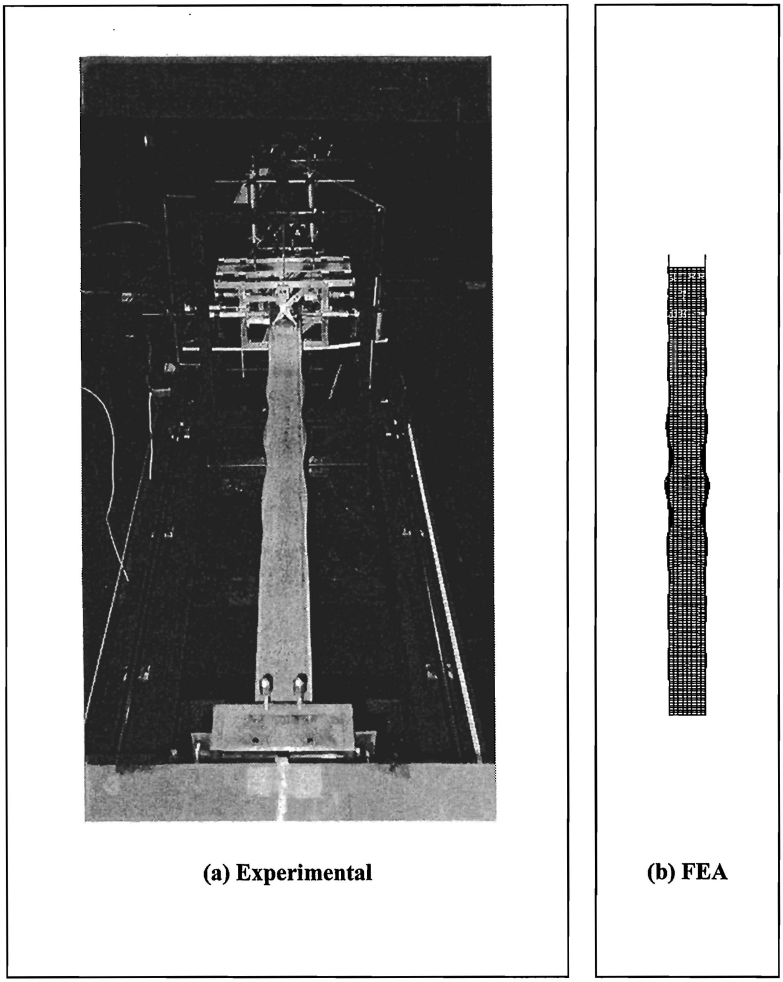

(a) Experimental

(b) FEA

Fig. 6. Comparison of Experimental and FEA Deformed Shapes for Specimen P48F1850

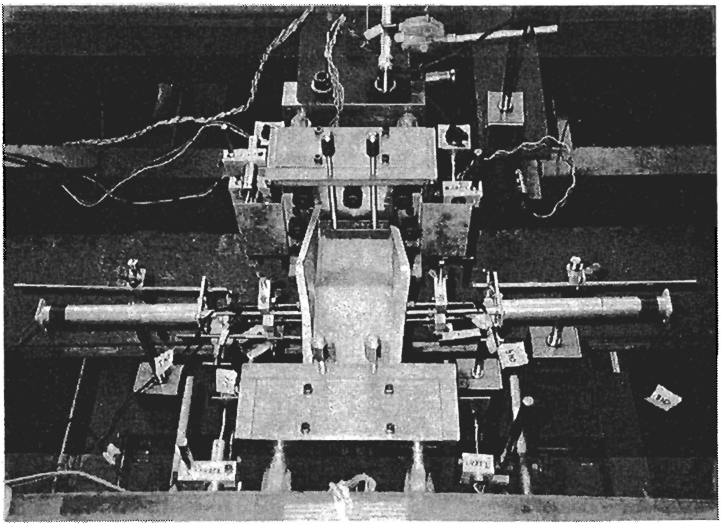

(a) Experimental

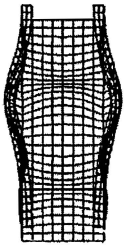

(b) FEA

Fig. 7. Comparison of Experimental and FEA Deformed Shapes for Specimen L48F0300

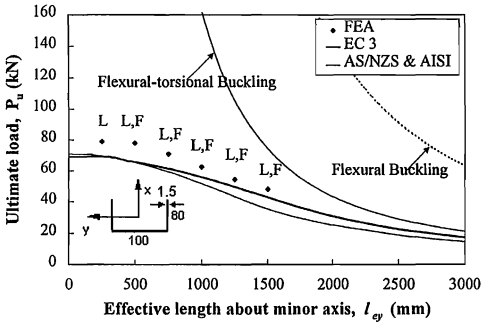

Fig. 8. Comparison of Proposed Column Strengths with Design Column Strengths for Series P1.5W100

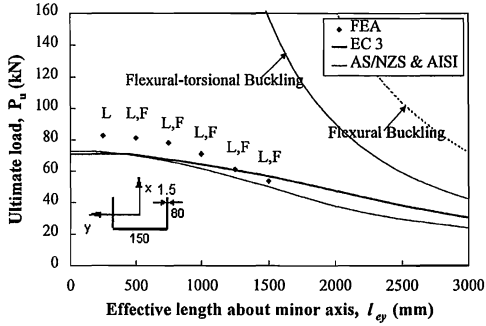

Fig. 9. Comparison of Proposed Column Strengths with Design Column Strengths for Series P1.5W150

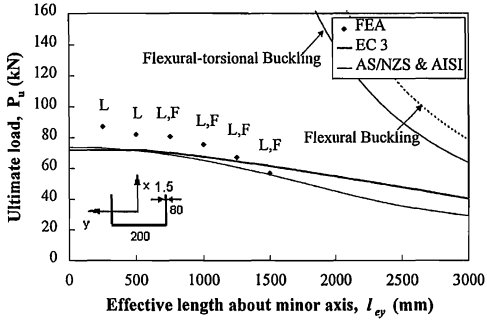

Fig. 10. Comparison of Proposed Column Strengths with Design Column Strengths for Series P1.5W200

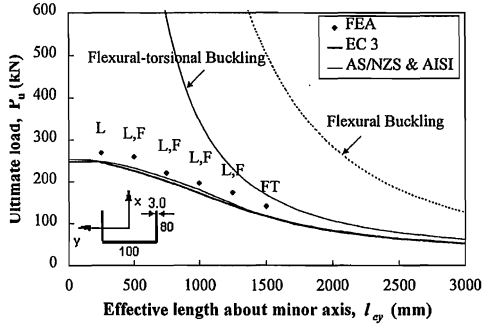

Fig. 11. Comparison of Proposed Column Strengths with Design Column Strengths for Series P3.0W100

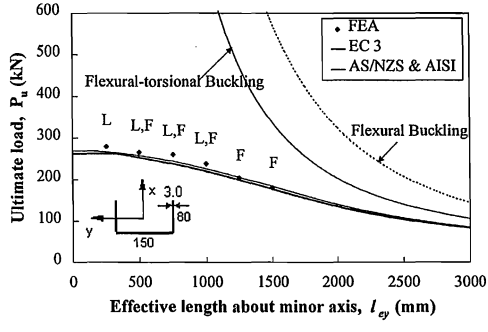

Fig. 12. Comparison of Proposed Column Strengths with Design Column Strengths for Series P3.0W150

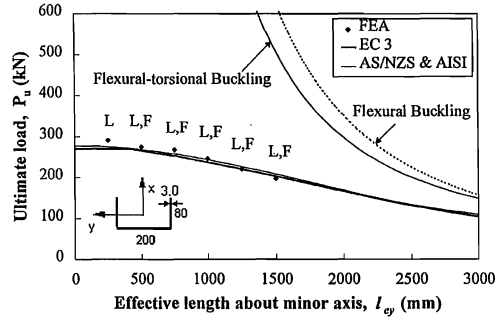

Fig. 13. Comparison of Proposed Column Strengths with Design Column Strengths for Series P3.0W200

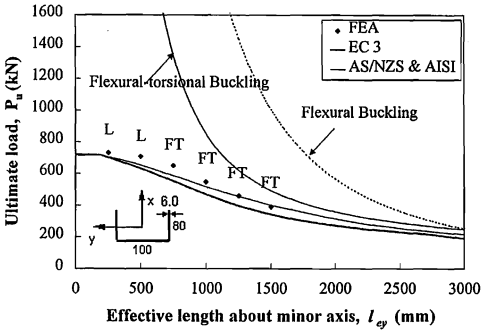

Fig. 14. Comparison of Proposed Column Strengths with Design Column Strengths for Series P6.0W100

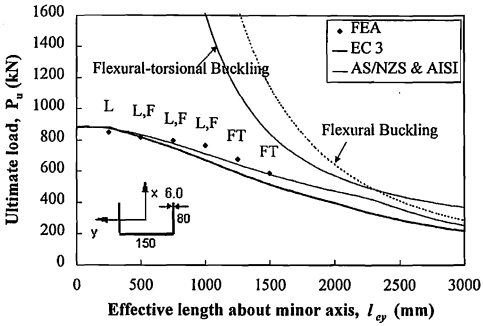

Fig. 15. Comparison of Proposed Column Strengths with Design Column Strengths for Series P6.0W150

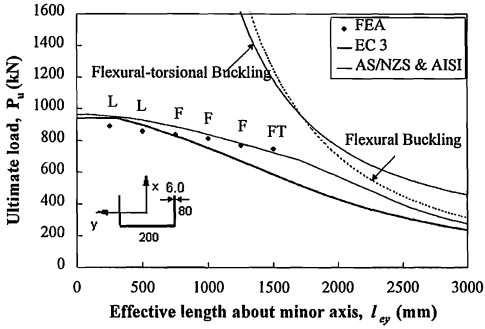

Fig. 16. Comparison of Proposed Column Strengths with Design Column Strengths for Series P6.0W200

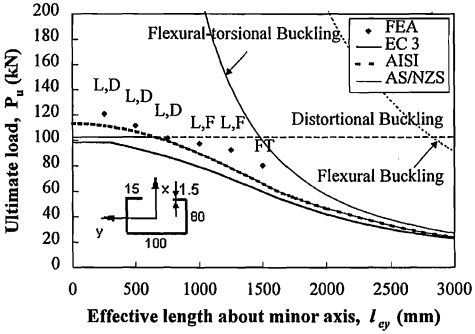

Fig. 17. Comparison of Proposed Column Strengths with Design Column Strengths for Series L1.5W100

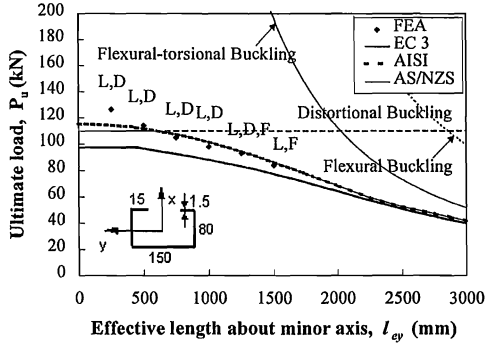

Fig. 18. Comparison of Proposed Column Strengths with Design Column Strengths for Series L1.5W150

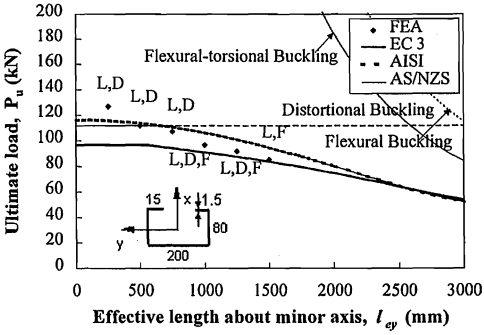

Fig. 19. Comparison of Proposed Column Strengths with Design Column Strengths for Series L1.5W200

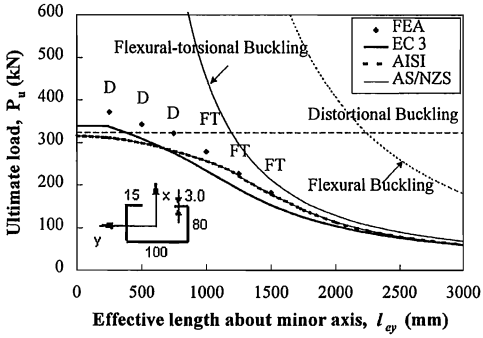

Fig. 20. Comparison of Proposed Column Strengths with Design Column Strengths for Series L3.0W100

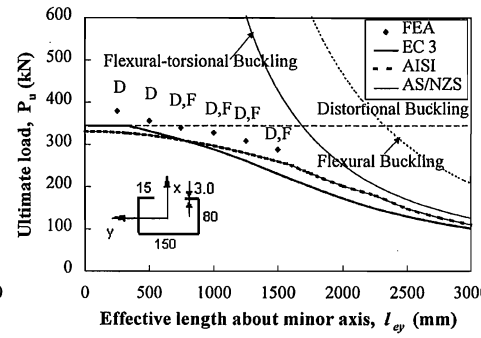

Fig. 21. Comparison of Proposed Column Strengths with Design Column Strengths for Series L3.0W150

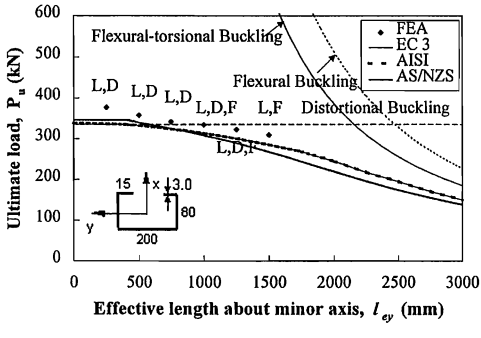

Fig. 22. Comparison of Proposed Column Strengths with Design Column Strengths for Series L3.0W200

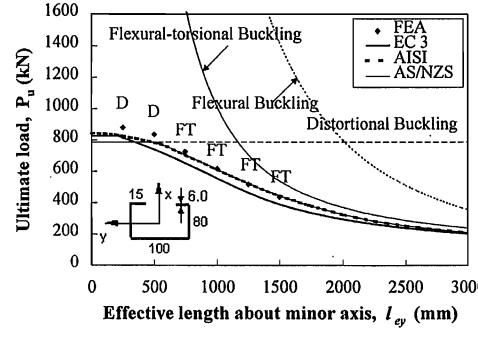

Fig. 23. Comparison of Proposed Column Strengths with Design Column Strengths for Series L6.0W100

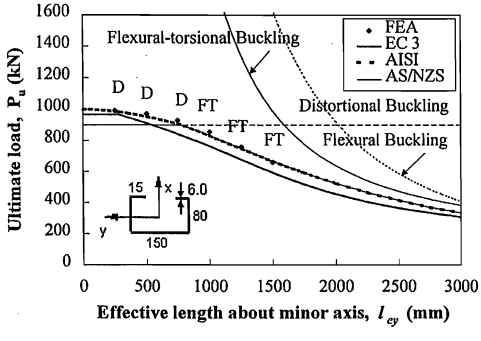

Fig. 24. Comparison of Proposed Column Strengths with Design Column Strengths for Series L6.0W150

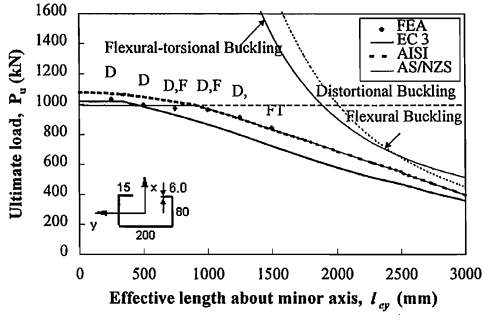

Fig. 25. Comparison of Proposed Column Strengths with Design Column Strengths for Series L6.0W200

Test series	Lips	Flanges	Web	Thickness		Radius	Area
	B_l	B_f	B_w	t	t^*	r_i	A
	(mm)	(mm)	(mm)	(mm)	(mm)	(mm)	(mm^2)
P36	N/A	36.8	96.9	1.51	1.47	0.85	247
P48	N/A	49.6	95.4	1.52	1.47	0.85	282
L36	12.5	37.0	97.3	1.52	1.48	0.85	280
L48	12.2	49.0	97.1	1.51	1.47	0.85	314

Note: 1 in. = 25.4 mm

* Base metal thickness

Table 1. Average Measured Specimen Dimensions

Test series	Nominal	Measured				
	$\sigma_{0.2}$	E	$\sigma_{0.2}$	$\sigma_{0.5}$	σ_u	ε_u
	(MPa)	(GPa)	(MPa)	(MPa)	(MPa)	(%)
P36	450	210	550	560	570	10
P48	450	210	510	525	540	11
L36	450	210	515	525	540	11
L48	450	200	550	560	570	10

Note: 1 ksi = 6.89 MPa

Table 2. Nominal and Measured Material Properties

Specimen	Experimental	Comparison													
		100%		75%		50%		25%		5%		2%		0.02%	
	P_{EXP} (kN)	P_{EXP}/P_{FEA}	P_{EXP}/P_{FEA}^*	P_{EXP}/P_{FEA}	P_{EXP}/P_{FEA}^*	P_{EXP}/P_{FEA}	P_{EXP}/P_{FEA}^*	P_{EXP}/P_{FEA}	P_{EXP}/P_{FEA}^*	P_{EXP}/P_{FEA}	P_{EXP}/P_{FEA}^*	P_{EXP}/P_{FEA}	P_{EXP}/P_{FEA}^*	P_{EXP}/P_{FEA}	P_{EXP}/P_{FEA}^*
P36F0280	65.0	0.91	0.96	0.90	0.95	0.89	0.95	0.90	0.96	0.89	0.95	0.89	0.95	0.68	0.73
P36F1000	59.0	0.97	1.04	0.96	1.03	0.95	1.02	0.94	1.02	0.94	1.01	0.94	1.01	0.67	0.72
P36F1500	50.1	1.03	1.12	1.01	1.10	0.99	1.08	0.97	1.06	0.96	1.04	0.95	1.04	0.61	0.66
P36F2000	41.7	1.23	1.35	1.17	1.28	1.08	1.19	1.01	1.11	0.94	1.03	0.92	1.01	0.69	0.76
P36F2500	32.8	0.83	0.92	0.83	0.92	0.82	0.91	0.83	0.92	0.82	0.91	0.82	0.91	0.81	0.90
P36F3000	24.7	0.98	1.11	0.95	1.07	0.94	1.05	0.91	1.03	0.90	1.01	0.89	1.01	0.89	1.00
	Mean	0.99	1.08	0.97	1.06	0.95	1.03	0.93	1.01	0.91	0.99	0.90	0.99	0.73	0.80
	COV	0.135	0.139	0.119	0.122	0.094	0.096	0.067	0.067	0.055	0.052	0.054	0.049	0.144	0.163

P_{FEA}*: Proposed column strength

Note: 1 kip = 4.45 kN

Table 3. Sensitivity Analysis of Column Strengths Based on Measured Geometric Imperfections

Specimen	Experimental	Comparison													
		100%		75%		50%		25%		5%		2%		0.02%	
	P_{EXP} (kN)	P_{EXP}/P_{FEA}	P_{EXP}/P_{FEA}^*	P_{EXP}/P_{FEA}	P_{EXP}/P_{FEA}^*	P_{EXP}/P_{FEA}	P_{EXP}/P_{FEA}^*	P_{EXP}/P_{FEA}	P_{EXP}/P_{FEA}^*	P_{EXP}/P_{FEA}	P_{EXP}/P_{FEA}^*	P_{EXP}/P_{FEA}	P_{EXP}/P_{FEA}^*	P_{EXP}/P_{FEA}	P_{EXP}/P_{FEA}^*
P36F0280	65.0	0.91	0.96	0.90	0.95	0.89	0.95	0.90	0.96	0.89	0.95	0.89	0.95	0.68	0.73
P36F1000	59.0	0.97	1.05	0.96	1.04	0.95	1.03	0.95	1.02	0.94	1.01	0.94	1.01	0.67	0.72
P36F1500	50.1	1.09	1.18	1.06	1.15	1.03	1.12	0.99	1.08	0.96	1.04	0.95	1.04	0.61	0.66
P36F2000	41.7	1.23	1.36	1.17	1.29	1.11	1.22	1.03	1.13	0.94	1.03	0.92	1.01	0.69	0.76
P36F2500	32.8	0.83	0.92	0.82	0.92	0.82	0.91	0.83	0.92	0.82	0.91	0.83	0.92	0.81	0.90
P36F3000	24.7	0.96	1.08	0.94	1.06	0.93	1.04	0.91	1.02	0.89	1.01	0.89	1.01	0.89	1.00
	Mean	1.00	1.09	0.98	1.07	0.96	1.04	0.93	1.02	0.91	0.99	0.91	0.99	0.73	0.79
	COV	0.144	0.146	0.126	0.128	0.107	0.108	0.076	0.075	0.057	0.053	0.048	0.044	0.145	0.164

P_{FEA}*: Proposed column strength

Note: 1 kip = 4.45 kN

Table 4. Sensitivity Analysis of Column Strengths Based on Plate Thickness

Specimen	Experimental	Comparison						
		100%	75%	50%	25%	5%	2%	0.02%
	e_{EXP}	$\frac{e_{EXP}}{e_{FEA}}$	$\frac{e_{EXP}}{e_{FEA}}$	$\frac{e_{EXP}}{e_{FEA}}$	$\frac{e_{EXP}}{e_{FEA}}$	$\frac{e_{EXP}}{e_{FEA}}$	$\frac{e_{EXP}}{e_{FEA}}$	$\frac{e_{EXP}}{e_{FEA}}$
	(mm)							
P36F0280	0.91	0.99	0.98	1.06	1.31	1.12	1.20	1.18
P36F1000	1.74	0.75	0.78	0.81	0.84	0.86	0.89	0.94
P36F1500	1.75	0.85	0.87	0.87	0.90	0.92	0.92	0.71
P36F2000	1.64	0.80	0.82	0.86	0.88	0.87	0.87	0.70
P36F2500	1.60	0.52	0.53	0.52	0.75	0.75	0.74	0.74
P36F3000	1.70	0.88	0.88	0.88	0.90	0.95	0.96	1.01
Mean		0.80	0.81	0.83	0.93	0.91	0.93	0.88
COV		0.198	0.190	0.209	0.208	0.132	0.165	0.219

Table 5. Sensitivity Analysis of Axial Shortenings Based on Measured Geometric Imperfections

Specimen	Experimental	Comparison						
		100%	75%	50%	25%	5%	2%	0.02%
	e_{EXP}	$\frac{e_{EXP}}{e_{FEA}}$	$\frac{e_{EXP}}{e_{FEA}}$	$\frac{e_{EXP}}{e_{FEA}}$	$\frac{e_{EXP}}{e_{FEA}}$	$\frac{e_{EXP}}{e_{FEA}}$	$\frac{e_{EXP}}{e_{FEA}}$	$\frac{e_{EXP}}{e_{FEA}}$
	(mm)							
P36F0280	0.91	0.99	0.98	1.06	1.31	1.12	1.20	1.18
P36F1000	1.74	0.75	0.77	0.80	0.84	0.86	0.89	0.93
P36F1500	1.75	0.79	0.81	0.84	0.87	0.92	0.92	0.71
P36F2000	1.64	0.80	0.82	0.85	0.87	0.87	0.87	0.70
P36F2500	1.60	0.52	0.52	0.53	0.75	0.74	0.83	0.74
P36F3000	1.70	0.88	0.88	0.88	0.90	0.96	0.96	1.02
Mean		0.79	0.80	0.83	0.92	0.91	0.94	0.88
COV		0.201	0.195	0.207	0.211	0.138	0.141	0.220

Table 6. Sensitivity Analysis of Axial Shortenings Based on Plate Thickness

Specimen	Experimental			FEA				Comparison		
	P_{EXP}	e_{EXP}	Failure Mode	P_{FEA}	P_{FEA}*	e_{FEA}	Failure Mode	P_{EXP} / P_{FEA}	P_{EXP} / P_{FEA}*	e_{EXP} / e_{FEA}
	(kN)	(mm)		(kN)	(kN)	(mm)				
P36F0280	65.0	0.91	L + F	72.0	68.0	0.70	L + F	0.90	0.96	1.31
P36F1000	59.0	1.74	L + F	62.4	58.0	2.08	L + F	0.95	1.02	0.84
P36F1500	50.1	1.75	L + F	50.4	46.4	2.00	L + F	0.99	1.08	0.87
P36F2000	41.7	1.64	F	40.6	36.9	1.88	F	1.03	1.13	0.87
P36F2500	32.8	1.60	F	39.6	35.6	2.14	FT	0.83	0.92	0.75
P36F3000	24.7	1.70	F	27.1	24.1	1.88	F	0.91	1.02	0.90
							Mean, P_m	0.93	1.02	0.92
							COV, V_p	0.076	0.075	0.211
							Safety Index, β	2.35	2.69	

P_{FEA}*: Proposed column strength

Note: 1 in. = 25.4 mm; 1 kip = 4.45 kN

Table 7. Comparison of Experimental and FEA Results for Series P36

Specimen	Experimental			FEA				Comparison		
	P_{EXP} (kN)	e_{EXP} (mm)	Failure Mode	P_{FEA} (kN)	P_{FEA}* (kN)	e_{FEA} (mm)	Failure Mode	P_{EXP} / P_{FEA}	P_{EXP} / P_{FEA}*	e_{EXP} / e_{FEA}
	(kN)	(mm)		(kN)	(kN)	(mm)				
P48F0300	66.0	0.84	L + F	71.0	67.0	1.01	L + F	0.93	0.98	0.83
P48F1000	62.7	2.01	L + F	67.8	63.1	2.65	L + F	0.92	0.99	0.76
P48F1500	55.5	2.08	L + F	56.8	52.3	2.46	L + F	0.98	1.06	0.85
P48F1850	47.2	1.98	L + F	49.8	46.5	2.35	L + F	0.95	1.02	0.84
P48F2100	43.6	2.06	L + F	44.0	40.0	2.43	L + F	0.99	1.09	0.85
P48F2500	38.5	1.98	L + F	38.1	34.3	2.16	L + F	1.01	1.12	0.92
P48F3000	37.4	2.35	L + F + FT	32.5	28.9	1.96	L + F	1.15	1.29	1.20
							Mean, P_m	1.00	1.08	0.89
							COV, V_p	0.080	0.099	0.162
							Safety Index, β	2.58	2.75	

P_{FEA}*: Proposed column strength

Note: 1 in. = 25.4 mm; 1 kip = 4.45 kN

Table 8. Comparison of Experimental and FEA Results for Series P48

Specimen	Experimental			FEA				Comparison		
	P_{EXP} (kN)	e_{EXP} (mm)	Failure Mode	P_{FEA} (kN)	P_{FEA}* (kN)	e_{FEA} (mm)	Failure Mode	P_{EXP} / P_{FEA}	P_{EXP} / P_{FEA}*	e_{EXP} / e_{FEA}
	(kN)	(mm)		(kN)	(kN)	(mm)				
L36F0280	100.2	0.86	L + D	101.5	100.9	0.83	L + D	0.99	0.99	1.03
L36F1000	89.6	2.19	L + D + F	96.8	94.9	2.37	L + D + F	0.93	0.94	0.92
L36F1500	82.4	2.46	L + F + FT	83.4	80.9	2.77	L + F	0.99	1.02	0.89
L36F2000	70.1	2.49	L + F + FT	68.5	65.8	2.80	L + F	1.02	1.07	0.89
L36F2500	58.1	2.52	F + FT	57.4	54.5	2.52	F + FT	1.01	1.07	1.00
L36F3000	39.3	2.60	F + FT	43.8	41.2	3.07	F + FT	0.90	0.95	0.85
							Mean, P_m	0.97	1.01	0.93
							COV, V_p	0.051	0.052	0.077
							Safety Index, β	2.62	2.75	

P_{FEA}*: Proposed column strength

Note: 1 in. = 25.4 mm; 1 kip = 4.45 kN

Table 9. Comparison of Experimental and FEA Results for Series L36

Specimen	Experimental			FEA				Comparison		
	P_{EXP} (kN)	e_{EXP} (mm)	Failure Mode	P_{FEA} (kN)	P_{FEA}* (kN)	e_{FEA} (mm)	Failure Mode	P_{EXP} / P_{FEA}	P_{EXP} / P_{FEA}*	e_{EXP} / e_{FEA}
	(kN)	(mm)		(kN)	(kN)	(mm)				
L48F0300	111.9	0.99	L + D	120.5	119.8	0.86	L + D	0.93	0.93	1.16
L48F1000	102.3	2.16	L + D	103.9	101.8	2.14	L + D	0.98	1.00	1.01
L48F1500	98.6	2.83	L + D + FT	101.9	98.8	3.15	L + D	0.97	1.00	0.90
L48F2000	90.1	3.12	L + D + FT	94.1	90.3	3.75	L + F	0.96	1.00	0.83
L48F2500	73.9	2.97	F + FT	68.6	65.2	2.77	F + FT	1.08	1.13	1.07
L48F3000	54.3	2.75	F + FT	51.8	48.7	2.66	F + FT	1.05	1.12	1.03
							Mean, P_m	0.99	1.03	1.00
							COV, V_p	0.057	0.075	0.117
							Safety Index, β	2.68	2.72	

P_{FEA}*: Proposed column strength

Note: 1 in. = 25.4 mm; 1 kip = 4.45 kN

Table 10. Comparison of Experimental and FEA Results for Series L48

Series	No. of Columns	P_{FEA}* / $P_{AS/NZS}$			P_{FEA}* / P_{EC3}		
		Mean	COV	Safety Index	Mean	COV	Safety Index
		P_m	V_p	β	P_m	V_p	β
P1.5W100	6	1.22	0.052	3.52	1.14	0.028	2.91
P1.5W150	6	1.13	0.036	3.31	1.09	0.084	2.48
P1.5W200	6	1.13	0.056	3.20	1.10	0.093	2.46
P3.0W100	6	1.12	0.053	3.18	1.15	0.046	2.89
P3.0W150	6	1.03	0.033	2.92	1.06	0.030	2.60
P3.0W200	6	1.01	0.041	2.80	1.03	0.038	2.47
P6.0W100	6	1.05	0.048	2.93	1.14	0.043	2.85
P6.0W150	6	1.02	0.040	2.86	1.08	0.074	2.49
P6.0W200	6	0.97	0.041	2.63	1.07	0.118	2.21

Table 11. Comparison of Proposed Column Strengths with Design Column Strengths for Plain Channels

Series	No. of Columns	P_{FEA}* / $P_{AS/NZS}$			P_{FEA}* / P_{AISI}			P_{FEA}* / P_{EC3}		
		Mean	COV	Safety Index	Mean	COV	Safety Index	Mean	COV	Safety Index
		P_m	V_p	β	P_m	V_p	β	P_m	V_p	β
L1.5W100	6	1.13	0.065	2.94	1.11	0.069	3.03	1.25	0.058	3.17
L1.5W150	6	1.02	0.070	2.50	1.01	0.053	2.74	1.16	0.066	2.81
L1.5W200	6	0.97	0.093	2.21	0.96	0.078	2.45	1.12	0.095	2.53
L3.0W100	6	1.10	0.066	2.85	1.10	0.066	3.04	1.16	0.036	2.96
L3.0W150	6	1.11	0.020	3.06	1.11	0.020	3.27	1.14	0.060	2.79
L3.0W200	6	1.08	0.021	2.94	1.08	0.020	3.15	1.09	0.036	2.71
L6.0W100	6	1.03	0.051	2.66	1.02	0.036	2.88	1.11	0.014	2.84
L6.0W150	6	1.04	0.037	2.72	1.01	0.014	2.88	1.09	0.038	2.69
L6.0W200	6	1.01	0.021	2.64	0.98	0.028	2.73	1.08	0.063	2.57

Table 12. Comparison of Proposed Column Strengths with Design Column Strengths for Lipped Channels